Adhesion and Cellular Compatibility of Silicone-Based Skin Adhesives

Sarah C. L. Fischer, Klaus Kruttwig, Vera Bandmann, René Hensel, Eduard Arzt*

Pressure-sensitive adhesives based on silicone materials have emerging potential as adhesives in healthcare products, in particular for gentle skin adhesives. To this end, adhesion to rough skin and biocompatibility are crucial factors for a successful implementation. In this study, the mechanical, adhesive, and biological properties of the two-component poly(dimethylsiloxane) Soft Skin Adhesive MG 7-9800 (SSA, Dow Corning) have been investigated and compared to Sylgard 184. Different mixing ratios of SSA's components allow for tuning of the shear modulus, thereby modifying the adhesive properties of the polymer. To give a comprehensive insight, the authors have analyzed the interplay between pull-off stress, adhesion energy, and stretch of the adhesive films on smooth and rough surfaces. The focus is placed on the effects of substrate roughness and on low pressure oxygen plasma treatment of the adhesive films. SSA shows superior biocompatibility in in vitro cell culture experiments. High pull-off stresses in the range of 3 N cm^{-2} on a rough surface are achieved, promising broad application spectra for SSA-based healthcare products.

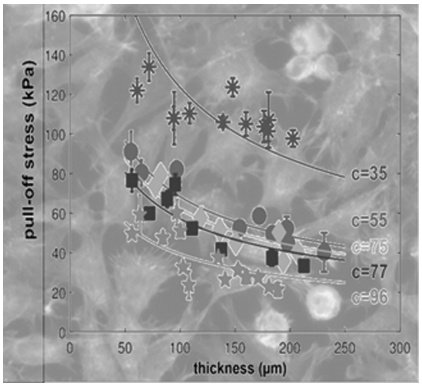

1. Introduction

Skin adhesives are essential in medical therapies and diagnostics as they provide secure placement of wound dressing, catheters, extensions, or electrodes.[1,2] Pressure-sensitive adhesives (PSAs) are widely used due to their ability to adhere to skin with small applied pressure and a short contact time.[3,4] Several studies focused on the investigation of mechanical and adhesive behavior of PSAs from natural or synthetic origin, including research on delamination phenomena.[5–10] The adhesive properties of PSAs can be varied by, e.g., the incorporation of different monomers during the polymerization process.[11] The modification of the viscoelastic properties of different materials directly influences their pull-off (tack) and peel strength to yield optimum properties for a wide field of applications including surface protection or medicine.[12–15] The three major classes of PSAs are acrylics, polyisobutylenes, and silicones.[16]

Acrylate-based PSA polymer systems dominate the market for medical adhesives due to their typical high adhesion strength.[17] However, the strong adhesion induced by acrylate formulations may induce irritations or even damage to the outermost skin layers during removal of the adhesive.[18–20] Thus, alternatives for gentle skin attachment are needed, particularly for sensitive skin of neonates or hardly regenerating skin of elderly people.[20–22] Another class of PSAs is silicones, exhibiting unique

S. C. L. Fischer, Dr. K. Kruttwig, Dr. V. Bandmann,[+]
Dr. R. Hensel, Prof. Dr. E. Arzt
INM—Leibniz Institute for New Materials
Campus D2 2, 66123 Saarbrücken, Germany
E-mail: eduard.arzt@leibniz-inm.de
S. C. L. Fischer, Prof. Dr. E. Arzt
Department of Materials Science and Engineering
Saarland University
Campus D2 2, 66123 Saarbrücken, Germany
[+]Present address: Department of Biology, Technical University Darmstadt, Schnittspahnstrasse 10, 64287 Darmstadt, Germany

Macromol. Mater. Eng. **2017**, *302*, 1600526

DOI: 10.1002/mame.201600526

adhesion characteristics to surfaces of both high and low surface energy and showing low initial tack and adhesion. Silicones are a versatile class of polymeric material, showing a low surface energy of 20 mJ m^{-2} and a high flexibility of the silicone network.[23] One of the most used silicone elastomers is poly(dimethyl siloxane) (PDMS), which exhibits a broad application spectrum in adhesive and biomedical technology. It has been widely used for medical devices, contact lenses manufacture, and cell culture purposes including lab-on-a-chip applications.[24] Its low surface reactivity, surface free energy, and the relatively high amount of low-molecular weight components cause PDMS to generate poor adhesion joints leading to the risk of adhesion failure.[25] One possible modification to increase the free surface energy of PDMS and hence its pull-off strength on smooth substrates[25] is the treatment with low-pressure plasma. This versatile technique, which is also one of the most frequently applied[26] techniques to increase the hydrophilic properties, results in a decreased adsorption of molecules to the surface, while promoting cellular attachment and cellular spreading behavior.[25] The Young's modulus of PDMS can be varied to below 1 MPa as it is a function of the cross linker concentration and/or the curing time.[27,28] For Sylgard 184 the manufacturer's recommendation is a ratio of 10:1 for the elastomer base to crosslinker ratio. The crosslinker concentration has been subsequently decreased to 50:1 in order to produce softer gels with Young's moduli around 50 kPa.[27,29] Because of these physiologically relevant Young's modulus values, such elastomers have great potential in cell culture research application.[29] Both parameters may influence the interaction between cells and polymer. Little research has been conducted so far with a view to a comprehensive and systematic investigation and optimization of the adhesive properties of silicone elastomers in response to surface roughness parameters.[30] Additionally, a direct comparison of different polymers with respect to their biocompatibility, adhesive properties, and physiologically relevant Young's modulus has scarcely been reported in literature.[31]

Here, we focused on the characterization of the adhesive behavior of Sylgard 184 and Soft Skin Adhesive (SSA) MG 7-9800 depending on the roughness of the substrate and as a function of low pressure oxygen plasma treatment. Additionally, in vitro adhesion and cytotoxicity effects of L929 murine fibroblasts on the two PSAs were analyzed in detail.

2. Materials and Methods

2.1. Preparation of Polymer Samples

Thin polymer films of two different PDMS formulations were manufactured: SSA MG 7-9800 (Dow Corning, Midland, MI, USA) and Sylgard 184 (Dow Corning, Midland, MI, USA). Different mixing ratios of the two components of SSA MG 7-9800 were produced to yield polymers with different mechanical properties. The SSA prepolymer (50:50/47:53/45:55/40:60 weight parts of component A: component B) as well as the Sylgard 184 prepolymer (10 weight parts of the basement to 1 weight part of the curing agent) were degassed under vacuum for 3 min at 2000 rpm in a SpeedMixer (DAC600.2 VAC-P, Hauschild Engineering, Hamm, Germany). The prepolymer mixtures were placed onto a glass slide (Marienfeld, Lauda-Königshofen, Germany) that was previously activated with oxygen plasma for 2 min at 60% power (PICO plasma system, Diener electronic, Ebhausen, Germany). Films with various thicknesses ranging from 50 to 230 μm were prepared by the doctor blade technique using a film applicator (Erichsen, Hemer, Germany). All polymer films were cured at 95 °C for 60 min. The thickness of the polymer films was measured using an optical microscope (VHX-2000, Keyence, Osaka, Japan) with an accuracy of ±20 μm. In selected experiments, cured polymer films were post-treated by plasma activation in an argon/oxygen atmosphere for 2 min (parameters: Forward radio-frequency (FR) target 50 W; forward RF range 5 W; maximum reflected RF 5 W; O_2 gas flow 11.5 sccm; Ar gas flow 35.0 sccm; Solanus model 950, Gatan, Munich, Germany).

2.2. Adhesion Measurements

In adhesion experiments, normal forces were recorded with a load cell (3 N, Tedea-Huntleigh 1004, Vishay Precision Group, Basingstoke, UK) mounted on a custom-built setup (Figure 1A). As nominally flat probes, two different glass substrates were used (Figure 1B). Substrate #1 (designated as "smooth") exhibited a mean absolute roughness R_a = 0.006 μm, and a mean peak-to-valley profile roughness R_z = 0.041 μm, while for substrate #2 (designated as "rough"), R_a = 0.271 μm and R_z = 2.174 μm. The substrates exhibited a circular contact area of 3.2 mm^2 for the smooth and 6.7 mm^2 for the rough substrate. The roughness values of the substrates were measured using a stylus profilometer (Surfcom 1500SD3, Carl Zeiss, Ostfildern, Germany) and an atomic force microscope (JPK instruments AG, Berlin, Germany). Before measurement, the substrate was cleaned with ethanol or isopropanol. A camera and prism, mounted below the sample, were used to optically align the specimen and the substrate while observing initial contact. To maximize contact between both surfaces the setup was mounted on a pivotable table allowing misalignment angle adjustment.

For adhesion experiments, specimen and substrate were converged at a velocity of 30 μm s^{-1} until a maximum force was reached, corresponding to a compressive preload of 10 ± 2 kPa. After a hold time of 1 s, the

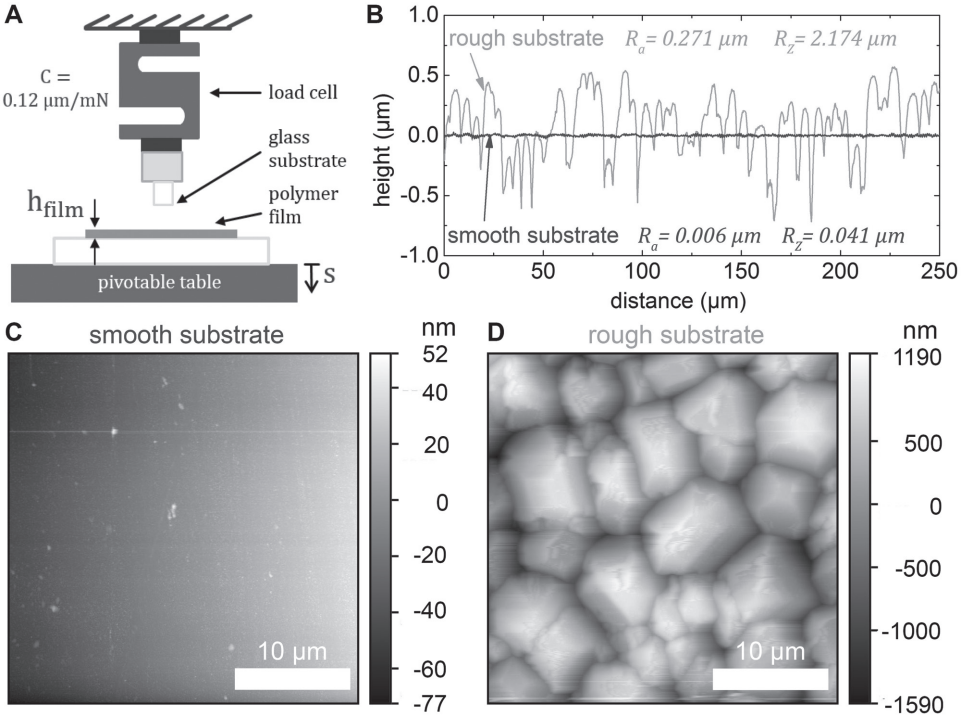

Figure 1. Experimental setup for adhesion testing. A) Schematic illustration of the adhesion measuring setup; h_{film} is the thickness of the silicone film and C is the machine compliance. B) Surface profiles of the smooth and rough substrate used as probes for the normal (tack) adhesion tests; R_a is the mean absolute roughness and R_z the mean peak-to-valley roughness. In addition, Atomic Force Microscopy (AFM) scans of the surface topography (30 µm × 30 µm) are shown for C) the smooth and D) the rough substrate.

specimen was withdrawn at a velocity of 10 µm s^{-1} until detachment. The measurements were repeated with different parameters at one position and three different positions on each individual specimen were tested. In selected measurements, the withdrawal velocity was changed from 2 to 50 µm s^{-1} or the hold time from 0 to 300 s.

Force, F, and displacement, s, were recorded. The displacement was corrected using the machine compliance (C = 0.12 µm mN^{-1}) to account for deformation of the setup. Values were then transformed into stress, $\sigma = F/A$, with the contact area, A, and relative displacement, $\varepsilon = (s - s_0)/h_{film}$, where h_{film} is the initial film thickness and s_0 is the displacement at which the force became zero and tensile deformation started. The maximum stress was defined as the pull-off stress, σ_{max}. The maximum relative displacement of the adhesive film, ε_{max}, was defined as the displacement at which detachment occurred.

The work of separation, W_{sep}, was calculated as follows

$$W_{sep} = \int_{s_o}^{s_{end}} \sigma \, ds \quad (1)$$

where s_{end} is the displacement at which the tensile stress returned to zero.

2.3. Materials Characterization

Frequency dependent storage, loss and complex shear moduli (G', G'', G^*) as well as the damping factor (tan δ) were determined using a rheometer Physica MCR-300 (Anton Paar, Graz, Austria) equipped with a cone/plate setup (diameter 25 mm, gap height 0.054 mm). The prepolymer mixtures were placed on the device, the plates approached and the polymer was cured at 90 °C for 30 min. Upon cooling to 25 °C, a frequency sweep from 0.01 to 100 Hz at constant amplitude of 0.1% was carried out.

2.4. Contact Angle Goniometry

The static water contact angle θ was measured using a goniometer (dataphysics, Filderstadt, Germany) by depositing a drop of 3 or 5 µL water with the needle inside the drop onto the surfaces, recording a side-view and subsequent image analysis.

2.5. Cell Culture Experiments

Murine mouse fibroblasts L929 were obtained from the American Type Culture Collection (Rockville, MS, USA) and cultured in Roswell Park Memorial Institute (RPMI) 1640 (Thermo Fisher Scientific, Dreieich, Germany)

supplemented with 10% fetal bovine serum and 1000 U mL^{-1} Penicillin and Streptomycin at 37 °C, 5% CO_2. Cells were routinely passaged with Accutase (Capricorn Scientific, Ebsdorfergrund, Germany) and cultured in sterilized tissue culture polystyrene flasks. For cell adhesion experiments, cells were seeded on glass slides coated with Sylgard 184 and SSA 50:50 on a mean surface area of 4.68 cm^2. Thickness of the polymer films was ≈150 µm. Polymer coated slides were placed for 24 h in phosphate buffered saline (PBS) before cell culture experiments. After 24 h culture period single cells were obtained by treatment with 0.25% trypsin-Ethylenediaminetetraacetic Acid (EDTA) solution. The cell number was determined using an automatic cell counter (CASY, OLS OMNI Life Science, Bremen, Germany) or a Neubauer chamber.

In order to characterize the cell cytotoxicity, release of lactate dehydrogenase (LDH) was measured with the CytoTox-ONE homogeneous membrane integrity assay (Promega, Madisson, WI, USA). Supernatant was removed from cells cultured for 24 h on polymeric materials and analyzed with a Tecan plate reader (Tecan, Crailsheim) according to manufacturer instructions. Cells were removed from the polymeric surface by brief incubation with trypsin. Fluorescence intensity was recorded at an excitation wavelength of 560 nm and an emission wavelength of 590 nm. As LDH positive control 9% TritonX-100 solution was added to cells cultured for 24 h on cell culture treated polystyrene. The initially seeded cell amount was 3×10^5 cells per well. Six independently performed experiments were used for statistical analysis. Additionally, trypan blue exclusion test was performed on $n = 3$ independently performed experiments. Two tailed students *t*-test was performed at a significance level of $\alpha = 0.05$, where indicated.

2.6. Immunofluorescence Analysis

Cells were fixated for 25 min with 4% paraformaldehyde and permeabilized with 0.25% TritonX-100 for 10 min. Blocking of unspecific antibody binding was reduced with a 60 min treatment of 5% bovine serum albumin (BSA) in PBS. Incubation with a 1:80 dilution of Phalloidin conjugated Alexa488 (Thermo Fisher Scientific) in PBS was performed over night at 4 °C. After an additional blocking step with 5% BSA cells were incubated with anti-α-tubulin (1:500, Sigma Aldrich) for 2 h at room temperature. As a secondary antibody, Alexa 546 (1:1000, Invitrogen) was used. For nuclear staining, cells were incubated with Hoechst Dye 33342 (1 µg mL^{-1}, Sigma) for 10 min and embedded with Aquamount (Polyscience, Eppelheim) in CELLVIEW cell culture dishes (Greiner bio-one). Microscopic analysis was performed with an inverted microscope (Leica, Wetzlar, Germany). Image brightness and contrast was adjusted with Leica LAS AF Lite software and ImageJ. Phase contrast images were acquired with a Zeiss inverted microscope.

2.7. Protein Adsorption Test

Sylgard 184, SSA 40:60, and SSA 50:50 exhibiting a thickness of 150 µm and mounted on glass slide were incubated with a solution of 1 mg mL^{-1} Fluorescein isothiocyanate (FITC) conjugated albumin (A9771, Sigma) for 3 h at 37 °C, 5% CO_2. After the incubation period, samples were subsequently washed with PBS and transferred to a new plate to minimize the influence of unspecific binding of albumin to the polystyrene surface during incubation. Fluorescence intensity was recorded with a Tecan plate reader. To correlate fluorescence intensity units to adsorbed protein amount, dilution series were performed and included in every measurement. The surface area of the samples was photographically documented, analyzed using ImageJ, and included in the calculation. Values are presented as microgram protein adsorbed to 1 cm^2 area.

3. Results and Discussion

3.1. Mechanical and Adhesion Properties

The dynamic-mechanical properties of Sylgard 184 and SSA MG 7-9800 in different mixing ratios, obtained from rheometer measurements, are shown in Figure 2. As a general observation for all materials, the storage (G'), loss (G''), complex (G^*) shear moduli as well as the damping factor ($\tan\delta$) increased with increasing frequency, hence, they became stiffer and more viscoelastic. The viscoelastic properties of SSA could be tuned by varying the mixing ratio from 50:50 to 40:60, which led to higher values of G', G'', and G^* and a lower damping factor. For example, G^* increased from 20 to 120 kPa (for 20 Hz) while $\tan\delta$ decreased from 0.75 to 0.2 when the mixing ratio was changed from 50:50 to 40:60. These results indicate that the cross-linking density of the polymer network increases and the mobility of polymer chains simultaneously decrease by changing the mixing ratio. Sylgard 184 exhibited a complex shear modulus of about 500 kPa (for 20 Hz), i.e., more than one order of magnitude higher than SSA 50:50. Furthermore, Sylgard 184 showed the lowest damping factor of only 0.1 at 20 Hz. Thus, Sylgard 184 is a rather elastic material at low frequencies, which is in line with literature.[32] The softest material analyzed in the current investigation, SSA 50:50, exhibits a much more pronounced viscoelastic characteristic that is reflected by a steep increase of the damping factor from 0.2 to 0.8 for a frequency sweep from 0.01 to 20 Hz.

The adhesive characteristics of polymer films, with uniform thicknesses ranging from 50 to 230 µm, of SSA MG 7-9800 in different mixing ratios and Sylgard 184 to

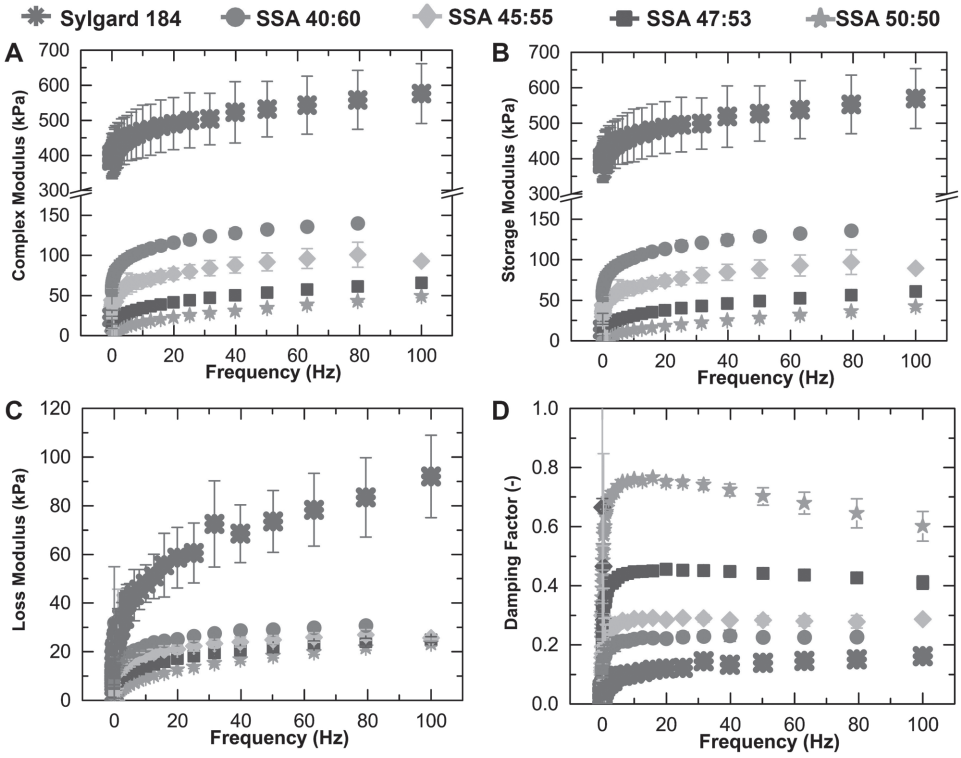

Figure 2. Determined material properties of the polymer materials from rheometer measurements. A) Complex, B) storage, and C) loss shear moduli as well as D) damping factor as a function of frequency. SSA 50:50 (stars), SSA 47:53 (squares), SSA 45:55 (diamonds), SSA 40:60 (circles), and Sylgard 184 (asterisk).

the smooth substrate are displayed in Figure 3. The following trends can be observed:

- Film thickness effect: For all materials, the pull-off stress increased with decreasing film thickness, t (Figure 3A). Particularly for the different SSAs, we obtained a two-fold increase of the pull-off stress for 50 μm thin films compared to the 230 μm thick films. This increase most likely corresponds to the scaling between interfacial and volume effects as in Chung and Chaudhury.[33] The authors propose that for very thin films, the pull-off stress is proportional to the function $\sigma_{max} = c \cdot \sqrt{E/t}$, where E is the Young's modulus; this is in good agreement with our data as shown by the fitting curves (Figure 3A). Based on the Young's modulus at 10 Hz, i.e., three times the shear modulus from rheometer measurements assuming a Poisson's ratio of $\nu = 0.5$, the coefficients c were evaluated and are displayed in Figure 3A.
- Modulus effect: A higher shear modulus resulted in higher pull-off stresses. For example, the pull-off stress increased from 55 kPa (SSA 50:50) to 90 kPa (SSA 40:60) and 120 kPa (Sylgard 184) for a constant film thickness of about 50 μm. The increase of the pull-off stress, σ_c, with increasing shear modulus is in accordance to Kendall's and Gent's models, according to which σ_c scales with $\sqrt{E}$.[34,35]
- Work of separation: The work of separation that similarly increased with thinner films as shown in Figure 3B. The highest values of about 3500 mJ m^{-2}, obtained for Sylgard 184, were twice as high as for the SSA mixtures 40:60, 45:55, and 47:53; the latter exhibit very similar values of up to 1750 mJ m^{-2} for 50 μm thick films. Only for the mixing ratio 50:50, values of up to 2500 mJ m^{-2} were obtained, most probably due to the high maximum relative displacement (Figure 3C).
- Maximum relative displacement: In contrast to all other materials, SSA 50:50 remained in contact with the smooth substrate up to 50% relative displacement for thicker films (200 μm) and 200% maximum relative displacement for thin films (50 μm). For SSA 47:53 and SSA 45:55, a transition from almost zero to about 30% maximum relative displacement was observed for films with a thickness of 120 and 200 μm, respectively. Thus, the transition is shifted toward higher film thickness with increasing shear modulus. For SSA 40:60 and Sylgard 184, the maximum relative displacement was almost zero for all films.
- Detachment mechanism: The maximum relative displacement appears to be connected with the detachment mechanisms observed. Instead of detaching abruptly from the edge, SSA 50:50 shows a rather ductile detachment. Cavitation and finger cracks are

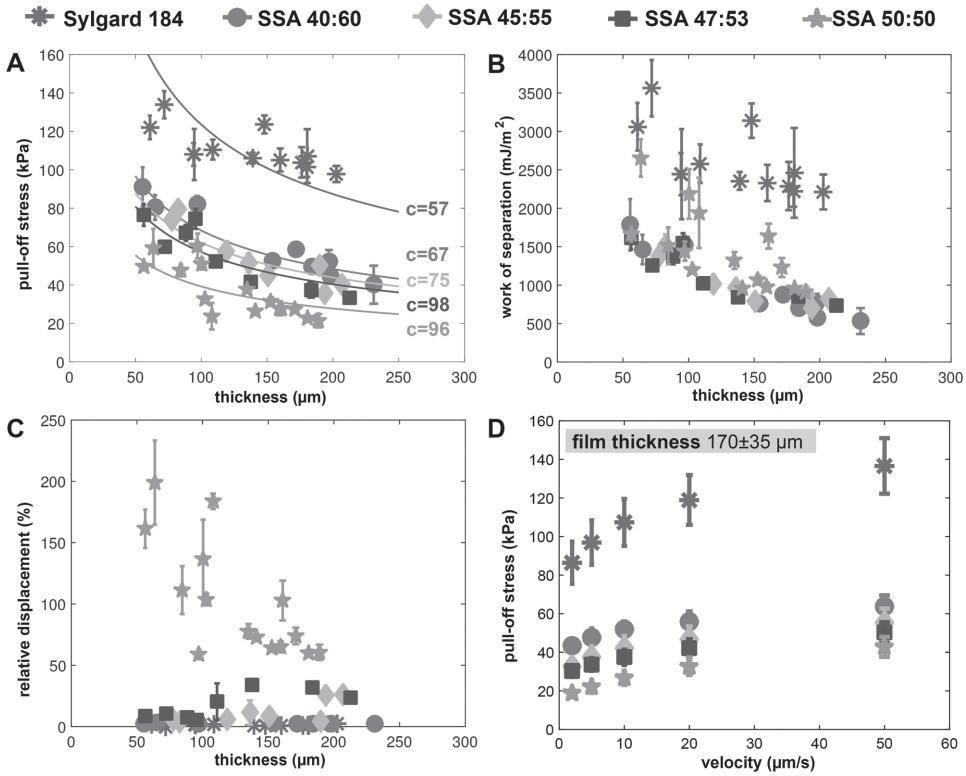

Figure 3. Adhesion measurements on the smooth substrate as a function of film thickness and pull-off velocity. A) Pull-off stress, B) adhesion energy, and C) maximum relative displacement as function of the film thickness of SSA 50:50 (stars), SSA 47:53 (squares), SSA 45:55 (diamonds), SSA 40:60 (circles), and Sylgard 184 (asterisk). The solid curves in (A) indicate the fit function $\sigma_{max} = c \cdot \sqrt{E \cdot t^{-1}}$ where c is the fit coefficient (see main text). The pull-off velocity for these measurements was 10 µm s^{-1}. D) Pull-off stress as a function of pull-off velocity for polymer films with a thickness in the range 170 ± 35 µm.

initiated throughout the contact area and the material deforms over a large displacement range, forming long threads between substrate and indenter.[36,37] This effect is, however, less pronounced, as the film thickness or elastic modulus increases.[38,39]

The adhesion measurements presented above were all carried out at a constant pull-off velocity of 10 µm s^{-1}. Additional measurements with different velocities ranging from 2 to 50 µm s^{-1} were performed for thicker film with 170 ± 35 µm (Figure 3D). Higher velocities resulted in higher pull-off stresses for all materials. For SSA 50:50, the pull-off stress increased by almost 100% from 20 to 40 kPa; the relative increase was less prominent as the storage shear modulus increased and the damping factor decreased, i.e., for SSA 40:60 and Sylgard 184. These results reflect the various viscoelastic properties of the materials as obtained from the rheometer measurements (Figure 2). SSA 50:50 exhibits the highest damping factor and therefore the highest sensitivity to the testing velocity. In contrast, Sylgard 184 has the lowest damping factor, but the pull-off strength still varied with velocity in accordance with a previous report.[32]

In summary, the mechanical properties of SSA could be tuned by varying the mixing ratio from 50:50 to 40:60, which strongly affected the adhesive properties. Sylgard 184, SSA 40:60, and SSA 50:50 showed a clearly distinguishable behavior in the adhesion experiments on the smooth substrate. Therefore, we restricted the further investigations to these three materials.

3.2. Biological Properties

Next, we present experiments relevant for the biological characterization of the materials. To enhance biocompatibility of the hydrophobic polymers two principle methods, protein adsorbance and oxygen plasma treatment were explored. Sylgard 184, SSA 40:60, and SSA 50:50 were incubated with FITC-conjugated albumin to visualize protein adsorption. No statistical significant difference in the adsorption of FITC conjugated BSA could be discriminated between the tested polymeric materials (Figure S1, Supporting Information). We detected 2.46 ± 0.37 µg cm^{-2} on Sylgard 184, 2.28 ± 0.32 µg cm^{-2} on SSA 50:50, and 2.39 ± 0.33 µg cm^{-2} on SSA 40:60 polymeric surfaces. The amount of protein coverage of surfaces depends amongst others,

Table 1. Water contact angle measurements. Contact angle of Sylgard 184, SSA 40:60, and SSA 50:50 was determined before (–) and after (+) oxygen plasma treatment.

Plasma treatment	Sylgard 184	SSA 40.60	SSA 50:50
–	117°	116°	136°
+	25°	21°	29°

on the bulk protein concentration to which the polymers have been exposed.[40] Protein surface densities ranging from 0.2 to 5 μg cm^{-2} have been reported.[40–43] The values we observed in the adsorption assay (Figure S1, Supporting Information) are comparable to previously reported data. The static water contact angles, tested before and after oxygen plasma treatment, for Sylgard 184 are shown in Table 1. They reveal the significant increase in surface energy after plasma treatment, in line with published results.[26] The initial static water contact angle of SSA 40:60 of 116° is comparable to the value obtained for Sylgard 184. Shifting the SSA ratio to 50:50 resulted in a significantly higher contact angle of 136°. This phenomenon has been reported for soft materials because of an elastic deformation due to capillary forces.[44]

To test the cellular adherence, L929 cells were cultured for 24 h on Sylgard 184, SSA 50:50, and Sylgard 184, SSA 50:50 treated with plasma. Independent of the polymer, significantly more cells adhered to the plasma treated surfaces, while no statistically relevant difference was found between both polymers (Figure 4A).

To determine cellular cytotoxic effects of the materials, release of LDH was analyzed after 24 h culture period (Figure 4B). The cytotoxicity on Sylgard 184 or SSA was comparable and not higher than on the Triton X-100 control (0.4% ± 1.8% cytotoxicity for cells cultured on Sylgard 184, 1.7% ± 1.9% cytotoxicity for cells cultured on plasma treated Sylgard 184, 1.7% ± 3.8% cytotoxicity for cells cultured on SSA 50:50 and 0.9% ± 3.1% cytotoxicity for cells cultured on plasma treated SSA 50:50) (Figure 4B). To further validate the results of the LDH determination, a trypan blue exclusion test as additional cytotoxicity assay was performed. We observed 1.2% ± 1.1% cytotoxicity for cells cultured on Sylgard 184, 1.2% ± 2.0% cytotoxicity for cells cultured on plasma treated Sylgard 184, 1.0% ± 0.9% cytotoxicity for cells cultured on SSA 50:50 and no cytotoxicity for cells cultured on plasma treated SSA 50:50. Therefore, we conclude that no statistically significant cytotoxicity was detectable while comparing both polymers to each other. In general, silicones are known for their low toxicity and high biostability, also in long-term applications.[45] However, polymeric materials may contain additional components, e.g., residual monomers or catalysts,[46] which might eventually influence physiological processes. Therefore, a cytotoxic evaluation with a specific cell line can be beneficial for further applications. Interestingly, In order to analyze the cellular adherence and cell spreading on the polymer surfaces, L929 cell was seeded for 24 h on both native, nonplasma treated polymers and polymers treated with oxygen plasma (Figure 4). Visualization of actin filaments and microtubules revealed the emanation of lamellipodia protrusions on native Sylgard 184 and SSA 50:50 elastomers (Figure 4C1,C2). We could not detect qualitative differences related to the cellular morphology while comparing both polymers. As expected, plasma treatment significantly improved cellular spreading on both surfaces resulting in remarkable extension of cellular body and lamellipodia protrusions (Figure 4C3,C4).

3.3. Comparison between Smooth and Rough Substrates

The results of the adhesion tests to smooth glass substrates (as shown in Figure 3) are not directly transferable to rough substrates, e.g., skin, which is our preferentially targeted application area. Several previous publications have already highlighted that roughness plays an important role in adhesion processes.[47,48] In addition, for biological testing purposes, all samples were plasma treated as it is a common method to increase cellular adhesion to plastic materials,[49,50] to sterilize materials and to make them more hydrophilic.[51] Additionally, it has been reported that plasma treatment leads to an increase in the root-mean-square roughness of polymers.[52] Thus, oxygen plasma treatment likely exerts fundamental effects onto adhesion properties and could influence the function of skin adhesives.

In Figure 5, the adhesion properties of Sylgard 184, SSA50:50, and SSA 40:60 films with a thickness between 170 ± 30 μm on the smooth and rough glass substrate are compared before and after plasma treatment. Pull-off stresses, adhesion energy as well as maximum relative displacement of Sylgard 184 and SSA 40:60 decrease significantly on the rough substrate compared to the smooth substrate without plasma treatment. For Sylgard 184 we observed a nearly 95% decrease in pull-off stress, while it is roughly 50% for SSA 40:60; SSA 50:50 shows lower, but comparable pull-off stress values on the smooth and the rough substrate (Figure 5A). Similar effects are seen in the adhesion energy values (Figure 5B), with one notable exception: SSA 50:50 exhibits a twofold increase in adhesion energy on the rough substrate, reaching values similar to Sylgard 184 on the smooth substrate. A similar maximum is seen in the maximum strain (Figure 5C). The impact of roughness on adhesion behavior is further illustrated in Figure S2 (Supporting Information). The detachment mechanisms remained similar on the rough substrate: Sylgard 184 and SSA 40:60 showed abrupt detachments, while SSA 50:50 remained in contact with the substrate for an extended time, detaching by fibrillation and withstanding

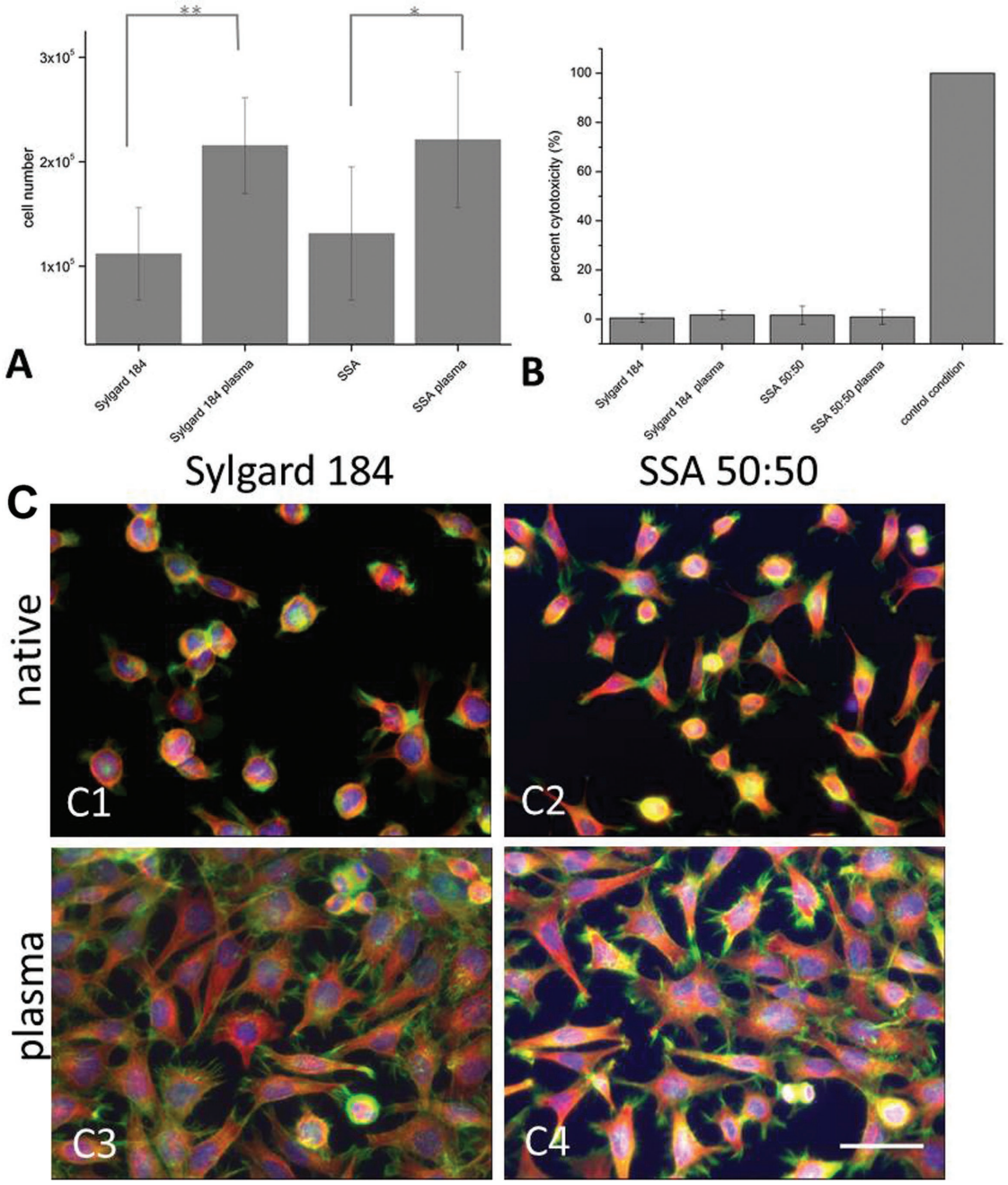

Figure 4. Cellular morphology after 24 h culture on polymeric surface. To determine cellular adhesion and assessment of cytotoxicity L929 cells were cultured for 24 h on PDMS, PDMS activated with plasma, SSA 50:50, and SSA 50:50 activated with plasma. A) Cell number attached to the different surfaces was determined. B) Release of lactate dehydrogenase was analyzed after release into the medium supernatant. As positive control for LDH release, cells were treated with 9% Triton X-100 solution. C) L929 cells were seeded for 24 h on C1) Sylgard 184 and C2) SSA 50:50. C3) Sylgard 184 plasma treated and C4) SSA 50:50 plasma treated. To visualize the actin cytoskeleton, fixated cells were incubated with FITC conjugated phalloidin (green). Additionally alpha tubulin was visualized (red). Nucleii were stained with Hoechst dye 33342 (blue). A,B) On native surfaces cells adhere poorly. Scale bars 25 μm. * denotes significance level $p < 0.05$, ** denotes significance level $p < 0.0005$.

high relative displacement (Figure S2, Supporting Information). Compared to the detachment of the investigated PSAs from smooth surfaces, where fewer, but larger cavitation areas were observed, higher nucleation frequency was generally more prevalent on a rough surface.

In these measurements, plasma treatment had no influence on the pull-off stress, the adhesion energy, and the maximum relative displacement on the smooth substrate for all tested materials. Interestingly, we observed a decrease of these values on the rough substrate, especially

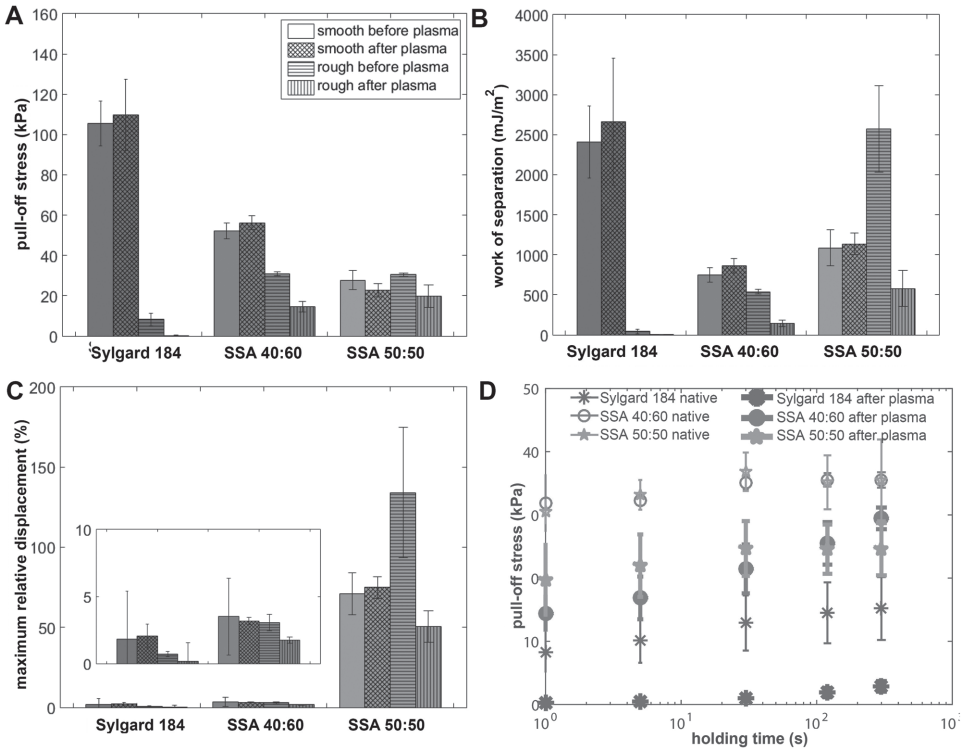

Figure 5. Comparison of the characteristic adhesion parameters obtained from smooth and rough substrates for Sylgard 184, SSA 40:60, and SSA 50:50 with and without plasma treatment. A) Pull-off stress, B) adhesion energy, and C) maximum relative displacement for experiments with a pull-off velocity of 10 μm s^{-1} and a hold time of 1 s. The inset is a close-up version of the data for Sylgard 184 and SSA 40:60 in (C). D) Influence of the hold time on the adhesion to the rough substrate. Only films with a thickness of 170 ± 35 μm were considered for this analysis.

for Sylgard 184 and SSA 40:60. Oxygen plasma treatment is commonly used to increase adhesion between PDMS and glass.[53] Furthermore, plasma treatment modifies the mechanical properties of the surface layer of polymers[54,55] as it results in the formation of an inorganic, wettable, brittle silica-like phase.[49,56] Presumably, this influences adhesion to the rough substrate as it reduces the adaptability to the surface.

The effect of the hold time on pull-off stress on the rough substrate is shown in Figure 5D. Pull-off stress increased with increasing hold time for not plasma-treated polymers but saturated at long hold times. In the case of plasma treated polymers, we observed a gradual increase of the pull-off stress with increasing hold time. A saturation of the pull-off stress was not reached in the evaluated time scale. When using a smooth substrate, the hold time did not greatly affect the results (not shown).

Depending on the particular application, different parameters may be controlling the adhesion performance. We conclude that combining all three parameters adequately describes the adhesion performance on complex surfaces and should therefore be included in the evaluation of dry adhesives.

In our study, we focused on the investigation of thin films composed of SSA 50:50, where pull-off stresses up to 3 N cm^{-2} could be reached on a rough substrate. The comparison of pull-off stresses between SSA 40:60 and SSA 50:50 implies almost no differences in adhesion as shown in Figure 5A.

However, adhesion energy and maximum relative displacement on rough surfaces are significantly higher for SSA 50:50 as visualized in Figure 5B,C. SSA 50:50's excellent adhesion performance on rough surfaces allows the development of novel adhesives for skin applications like wearable sensors.

4. Conclusions

The mechanical, adhesive, and biological properties of SSA have been investigated and compared to Sylgard 184 with a special focus on roughness and low pressure oxygen plasma treatment.

- No cytotoxic effects could be detected when culturing murine fibroblast on SSA surfaces and cellular adhesion was enhanced after plasma treatment.

- We have clearly shown that pull-off stress of the investigated Sylgard 184 and SSA 40:60 is highly dependent on the substrate type used, while almost no differences were observed, when focusing on SSA 50:50.
- Pull-off stress values can be expected to increase furthermore when the roughness increases, which makes this material very promising for applications as skin adhesive.
- Pull-off stress of SSA 50:50 was also not negatively affected by the treatment with oxygen plasma, therefore balancing biocompatibility and mechanical strength.

Supporting Information

Supporting Information is available from the Wiley Online Library or from the author.

Acknowledgements: S.C.L.F. and K.K. contributed equally to this work. The authors would like to acknowledge Angela Rutz with her assistance in performing the biological experiments. Katja Groß, Lukas Engel, Henrik Ollmann and Joachim Blau are acknowledged for their help in setting up and performing the adhesion experiments. The authors would like to thank Biesterfeld Spezialchemie GmbH (Hamburg, Germany), especially Robert Radsziwill, for continuous support and discussions. The research leading to these results had received funding from the European Research Council under the European Union's Seventh Framework Programme (FP/2007-2013)/ European Research Council (ERC) Grant Agreement No. 340929, Advanced Grant "Switch2Stick" to E.A. S.C.L.F., K.K., V.B., R.H., and E.A. contributed with conception and experimental design. S.C.L.F. and K.K. performed the experiments and carried out analysis of data. S.C.L.F., K.K., V.B., R.H., and E.A. wrote the paper.

Received: November 29, 2016; Revised: January 12, 2017; Published online: February 22, 2017; DOI: 10.1002/mame.201600526

Keywords: biocompatibility; oxygen plasma treatment; poly(dimethylsiloxane); pressure-sensitive adhesives; roughness

[1] M. K. Kwak, C. Pang, H. E. Jeong, H. N. Kim, H. Yoon, H. S. Jung, K. Y. Suh, *Adv. Funct. Mater.* **2011**, *21*, 3606.
[2] J. S. Kaiser, M. Kamperman, E. J. de Souza, B. Schick, E. Arzt, *Int. J. Artif. Organs* **2011**, *34*, 180.
[3] C. Creton, *MRS Bull.* **2011**, *28*, 434.
[4] C. Creton, L. Leibler, *J. Polym. Sci., Part B: Polym. Phys.* **1996**, *34*, 545.
[5] W. Maassen, M. A. R. Meier, N. Willenbacher, *Int. J. Adhes. Adhes.* **2016**, *64*, 65.
[6] R. Udagama, E. Degrandi-Contraires, C. Creton, C. Graillat, T. F. L. McKenna, E. Bourgeat-Lami, *Macromolecules* **2011**, *44*, 2632.
[7] Z. Czech, *Int. J. Adhes. Adhes.* **2004**, *24*, 119.
[8] S. Sun, M. Li, A. Liu, *Int. J. Adhes. Adhes.* **2013**, *41*, 98.
[9] H. Lakrout, P. Sergot, C. Creton, *J. Adhes.* **1999**, *69*, 307.
[10] J. Nase, A. Lindner, C. Creton, *Phys. Rev. Lett.* **2008**, *101*, 074503.
[11] D. A. Dimas, P. P. Dallas, D. M. Rekkas, N. H. Choulis, *AAPS PharmSciTech* **2000**, *1*, 80.
[12] H. S. Tan, W. R. Pfister, *Pharm. Sci. Technol. Today* **1999**, *2*, 60.
[13] F. Tokumura, T. Homma, T. Tomiya, Y. Kobayashi, T. Matsuda, *Skin Res. Technol.* **2007**, *13*, 211.
[14] J. Renvoise, D. Burlot, G. Marin, C. Derail, *Int. J. Pharm.* **2009**, *368*, 83.
[15] E. P. Chang, *J. Adhes.* **1997**, *60*, 233.
[16] R. Toddywala, Y. W. Chien, *J. Controlled Release* **1990**, *14*, 29.
[17] S. Venkatraman, R. Gale, *Biomaterials* **1998**, *19*, 1119.
[18] S. R. Mason, *Ostomy Wound Manage.* **1997**, *43*, 26.
[19] L. McNichol, C. Lund, T. Rosen, M. Gray, *Journal of Wound, Ostomy and Continence Nursing* **2013**, *40*, 365.
[20] B. Laulicht, R. Langer, J. M. Karp, *Proc. Natl. Acad. Sci. USA* **2012**, *109*, 18803.
[21] J. M. Karp, R. Langer, *Nature* **2011**, *477*, 42.
[22] G. J. Fisher, Z. Wang, S. C. Datta, J. Varani, S. Kang, J. J. Voorhees, *N. Engl. J. Med.* **1997**, *337*, 1419.
[23] S. K. Thanawala, M. K. Chaudhury, *Langmuir* **2000**, *16*, 1256.
[24] A. W. Lloyd, R. G. A. Faragher, S. P. Denyer, *Biomaterials* **2001**, *22*, 769.
[25] J. Roth, V. Albrecht, M. Nitschke, C. Bellmann, F. Simons, S. Zschoche, S. Michel, C. Luhmann, K. Grundke, B. Voit, *Langmuir* **2008**, *24*, 12603.
[26] S. H. Tan, N.-T. Nguyen, Y. C. Chua, T. G. Kang, *Biomicrofluidics* **2010**, *4*, 32204.
[27] D. Fuard, T. Tzvetkova-Chevolleau, S. Decossas, P. Tracqui, P. Schiavone, *Microelectron. Eng.* **2008**, *85*, 1289.
[28] Z. Wang, A. A. Volinsky, N. D. Gallant, *J. Appl. Polym. Sci.* **2014**, *131*, 41050.
[29] X. Q. Brown, K. Ookawa, J. Y. Wong, *Biomaterials* **2005**, *26*, 3123.
[30] V. Barreau, R. Hensel, N. K. Guimard, A. Ghatak, R. M. McMeeking, E. Arzt, *Adv. Funct. Mater.* **2016**, *26*, 4687.
[31] P. M. Van Midwoud, A. Janse, M. T. Merema, G. M. M. Groothuis, E. Verpoorte, *Anal. Chem.* **2012**, *84*, 3938.
[32] M. A. Meitl, Z.-T. Zhu, V. Kumar, K. J. Lee, X. Feng, Y. Y. Huang, I. Adesida, R. G. Nuzzo, J. A. Rogers, *Nat. Mater.* **2006**, *5*, 33.
[33] J. Y. Chung, M. K. Chaudhury, *J. Adhes.* **2005**, *81*, 1119.
[34] K. Kendall, *J. Phys. D: Appl. Phys.* **1971**, *4*, 320.
[35] A. N. Gent, *Rubber Chem. Technol.* **1974**, *47*, 202.
[36] A. J. Crosby, K. R. Shull, H. Lakrout, C. Creton, *J. Appl. Phys.* **2000**, *88*, 2956.
[37] C. Creton, M. Ciccotti, *Rep. Prog. Phys.* **2016**, *79*, 046601.
[38] R. E. Webber, K. R. Shull, A. Roos, C. Creton, *Phys. Rev. E* **2003**, *68*, 021805.
[39] J. Nase, O. Ramos, C. Creton, A. Lindner, *Eur. Phys. J. E* **2013**, *36*, 103.
[40] G. Toworfe, R. Composto, C. Adams, I. Shapiro, P. Ducheyne, *Departmental Papers (MSE)* **2003**, http://repository.upenn.edu/mse_papers/4.
[41] P. A. Dimilla, S. M. Albelda, J. A. Quinn, *J. Colloid Interface Sci.* **1992**, *153*, 212.
[42] J. B. Lhoest, E. Detrait, P. van den Bosch de Aguilar, P. Bertrand, *J. Biomed. Mater. Res.* **1998**, *41*, 95.
[43] A. Rezania, K. E. Healy, *Biotechnol. Prog.* **1999**, *15*, 19.
[44] A. Marchand, S. Das, J. H. Snoeijer, B. Andreotti, *Phys. Rev. Lett.* **2012**, *109*, 236101.
[45] Y. Wu, Q. Zhao, J. M. Anderson, A. Hiltner, G. A. Lodoen, C. R. Payet, *J. Biomed. Mater. Res.* **1991**, *25*, 725.

[46] E. Briganti, P. Losi, A. Raffi, M. Scoccianti, A. Munaò, G. Soldani, *J. Mater. Sci. Mater. Med.* **2006**, *17*, 259.
[47] A. Chiche, P. Pareige, C. Creton, *C. R. Acad. Sci., Ser. IV: Phys.* **2000**, *1*, 1197.
[48] B. N. J. Persson, S. Gorb, *J. Chem. Phys.* **2003**, *119*, 11437.
[49] M. J. Owen, P. J. Smith, *J. Adhes. Sci. Technol.* **1994**, *8*, 1063.
[50] C. F. Amstein, P. A. Hartman, *J. Clin. Microbiol.* **1975**, *2*, 46.
[51] C. Oehr, *Nucl. Instruments Methods Phys. Res., Sect. B* **2003**, *208*, 40.
[52] S. L. Peterson, A. McDonald, P. L. Gourley, D. Y. Sasaki, *J. Biomed. Mater. Res. A* **2005**, *72*, 10.
[53] B.-H. Jo, L. M. Van Lerberghe, K. M. Motsegood, D. J. Beebe, *J. Microelectromechan. Syst.* **2000**, *9*, 76.
[54] K. L. Mills, X. Zhu, S. Takayama, M. D. Thouless, *J. Mater. Res.* **2008**, *23*, 37.
[55] S. Pinto, P. Alves, C. M. Matos, A. C. Santos, L. R. Rodrigues, J. A. Teixeira, M. H. Gil, *Colloids Surf., B* **2010**, *81*, 20.
[56] D. W. Fakes, J. M. Newton, J. F. Watts, M. J. Edgell, *Surf. Interface Anal.* **1987**, *10*, 416.